ELSEVIER

Polymer 42 (2001) 6823–6831

polymer

www.elsevier.nl/locate/polymer

Phase behavior and molecular chain environment of organic–inorganic hybrid materials based on poly(*n*-butyl methacrylate-co-(3-(methacryloxypropyl)) trimethoxysilane)

Cheng-Kuang Chan, I-Ming Chu*

Department of Chemical Engineering, National Tsing Hua University, Hsinchu 300, Taiwan, ROC

Received 6 November 2000; received in revised form 22 January 2001; accepted 27 February 2001

Abstract

Hybrid materials based on poly(*n*-butyl methacrylate-co-(3-(methacryloxypropyl)) trimethoxysilane) were synthesized via a sol–gel process. From a phase behavior study of these hybrid materials using a differential scanning calorimeter (DSC) and solid-state nuclear magnetic resonance (NMR) spectroscopy, it was found that the hybrid system was miscible for organic and inorganic phases with low silane content, but exhibited heterogeneously when silane content was increased to 40 mol% or more. Furthermore, the hybrid system became more complicated when 50 mol% or more silane introduced. It was also found that an inorganic Si–O–Si network developed, which resulted in side chain segments into two different molecular environments and with different relaxation behaviors. The development of an inorganic matrix of a Si–O–Si structure and the corresponding polymer chain environment were also discussed in detail.

Keywords: Hybrid; Nuclear magnetic resonance; Heterogeneous

1. Introduction

The discovery of the extraordinary tendency of organosilicon compounds to form siloxane polymers containing organic side groups caused a sudden increase of activity in the late 1930s, which established a chemical and physical basis for understanding of the sol–gel process. This sol–gel technique was used initially for the production of inorganic glasses by polymerization of silicon alkoxides with two-steps networks forming process: hydrolysis and condensation with either acid or base catalyzed [1–5]. This technique has made great advances in the synthesis of novel organic–inorganic hybrid materials in the last two decades [6–10]. At the present time, sol–gel technology is been widely used and studied in industrial plants and laboratories. Besides, more and more novel hybrid materials synthesized via the sol–gel process have been developed for use in optical, electrical, sensor, and laser technologies. These applications often require hybrid materials with special properties such as transparency, homogeneity, and nano-scale composites. Hence, the phenomenon of phase separation between organic and inorganic phases is very important in order to develop suitable technology in these areas. Therefore, the compatibility of hybrid materials needs to be investigated thoroughly.

The measurement of glass transition temperature (T_g) is a useful method for investigating the miscibility of blend systems. The differential scanning calorimeter (DSC) [11,12], dynamic mechanical analyzer (DMA) [12,13], dilatometer, and dielectric relaxation are all powerful tools for conducting such work. However, T_g measurements can only give indication of homogeneity of a material on a scale not smaller than 150 Å. It is obvious that more information at a smaller scale is needed in order to understand blend systems in more detail. Once the conditions for miscibility on nano-scales can be resolved, the phase behavior of blends can then be controlled for different purposes.

In recent years, solid-state nuclear magnetic resonance (NMR) spectroscopy has been applied to the study of micro-heterogeneity in blend systems, following the pioneering works of McBrierty et al. [14] and Stejskal et al. [15]. The classic solid-state NMR technique used for studying the miscibility and molecular structural information of polymer blends on a molecular level is the analysis of the proton spin-lattice relaxation times in the rotating frame ($T_{1\rho,H}$) [16–19]. The value of $T_{1\rho,H}$ is related to the spin-diffusion process, with maximum path lengths of ca. 20 Å.

* Corresponding author. Tel.: +886-35-715-131; fax: +886-35-715-408.
E-mail address: imchu@che.nthu.edu.tw (I.-M. Chu).

0032-3861/01/$ - see front matter
PII: S0032-3861(01)00178-1

Thus, if the two components of the blend have the same $T_{1\rho,H}$ value, the system is miscible or the scale of the separated domains is smaller than 20 Å. In other words, they will have different spin relaxation rates from those obtained by solid-state NMR, if the two species of the system are incompatible. Undoubtedly, this interpretation is based on the assumption that the two components have different $T_{1\rho,H}$ values before blending. Therefore, if the designated chain segments in the system have unique chemical shifts, the responses of the segments can be monitored. Moreover, the proton relaxation behavior of the designated segments can be measured independently, and the phase behavior can also be determined.

Vinyl polymer modified organic–inorganic composite materials have been developed for several years [20,21]. In these materials, vinyl polymer chains are distributed in, and covalently bonded to, the inorganic matrix. While the sol–gel reaction is proceeding, phase separation may take place if the interfacial interaction between organic and inorganic phases is not strong enough. Thus, the miscibility of these systems can be further investigated by DSC and solid-state NMR to understand the phase behavior on different scales for various applications.

In this study, a new type of hybrid material with covalent bonds between organic and inorganic phases was developed. DSC and high resolution solid-state NMR were employed to estimate the T_g of the materials and the mobility of specific chain segments. The dependence of phase behavior on the ratio of organic–inorganic components will be discussed.

2. Experimental

2.1. Synthesis of polymer precursors

A mixture of monomers, *n*-butyl methacrylate (BMA, methacrylic acid *n*-butyl ester, TCI) and (3-(methacryloxypropyl)) trimethoxysilane (3-MPS, Z-6030, Dow Corning Company), with various mole ratios and toluene (90 g, as solvent), was charged into a four-necked reactor. After raising the temperature to 75°C, 2 wt% (based on the weight of all the monomers) of 2,2′-azobisisobutyronitrile (AIBN, Showa) was added and stirred under a nitrogen atmosphere for 10 h to synthesize the desired copolymers with different mole fractions of silane content as the hybrid material precursors. Most of the solvent in the mixtures was removed in a rotary evaporator. The copolymers were then precipitated using methanol in an ice bath, and the products were dried in a vacuum. The molecular weight of the synthesized copolymers was further determined by gel permeation chromatography with polystyrene as the standard; the eluent used was tetrahydrofuran (THF) with an elution rate of 1.0 ml/min.

2.2. Preparation of desired hybrid materials

The sol–gel process was carried out at 20°C in THF with hydrochloric acid (HCl) catalyzed and the reagent ratio of $H^+/H_2O/Si = 0.04/3/1$ (mole ration). The copolymers were dissolved in 10 g THF. Subsequently, the HCl/H_2O/THF solution (2 g THF) was added and mixed well. The samples were covered to reduce the evaporation rate of the solvent. After 48 h, the hybrid films were then heated at 40°C under vacuum for 24 h to remove any residual solvent and by-products (water and alcohol). The samples were aged 30 days at 40°C prior to being investigated further. In addition, a neat organic film was made from the homopolymer of BMA (p-BMA) in the absence of HCl, and H_2O was added.

2.3. T_g investigation by DSC

The T_g of synthesized hybrid materials was measured using a TA 2010 series DSC. Appropriate amounts of samples (ca. 5 mg) were sealed in aluminum sample pans and were prepared by compression molding at room temperature. DSC thermo-scans of the hybrid materials were then conducted under a dry nitrogen atmosphere at a heating rate of 20°C/min from −25 to 80°C.

2.4. Solid-state NMR spectroscopy

Bruker DSX-400 solid-state NMR was introduced to investigate the solid-state behavior of the desired hybrid materials. The spectra of ^{29}Si high power radio frequency decoupling were determined at 79.37 MHz. The ^{29}Si pulse length was 2 μs with a delay time of 5 s. Proton decoupled solid-state NMR spectra were acquired at 399.53 MHz for ^{1}H and 100.47 MHz for ^{13}C using cross polarization sequence and magic angle spinning (CP/MAS). The measurement of proton spin-lattice relaxation times in the rotating frame ($T_{1\rho,H}$) was measured with 4.2 μs π/2 ^{1}H pulse sequences and a 1.5 s delay time between the pulses. A contact time of 1 ms was used for cross polarization decoupling to the ^{13}C nuclei after a variable ^{1}H spin lock time. All the experiments were carried out at 300 K. The spinning rate of 7.00 kHz was used for all ^{29}Si and ^{13}C spectra to avoid overlapping of resonance lines.

3. Results and discussions

The molecular weight of synthesized BMA/3-MPS copolymers, which were the precursor of the sol–gel process, was determined by gel permeation chromatography. The average molecular weights ($\overline{Mn}$) and polydispersity ($\overline{Mw}/\overline{Mn}$) of all the synthesized copolymers are shown in Table 1, and are similar to each other. Subsequently, DSC and solid-state NMR were introduced to investigate the macroscopic and microscopic segmental dynamics of the organic–inorganic hybrid materials that are based on these copolymer precursors.

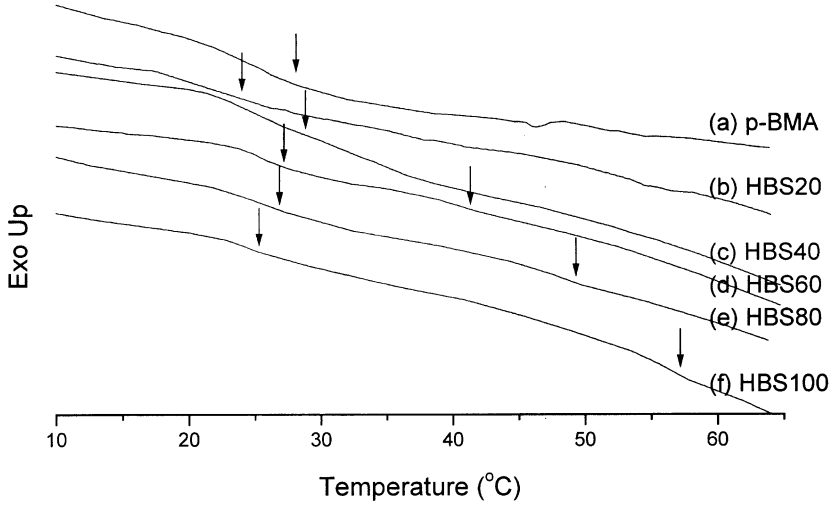

Fig. 1. Glass transition profiles of (a) p-BMA, (b) HBS20, (c) HBS40, (d) HBS60, (e) HBS80, and (f) HBS100, respectively. The glass transition temperatures were also denoted by arrows.

3.1. T_g investigation of desired hybrid materials by DSC

Fig. 1 displays the glass transition profiles of the BMA homopolymer and partially synthesized hybrid materials; the complete glass transition data and their appearance are shown in Table 2. In this table, it is indicated that the T_g of BMA homopolymer was 28.1°C. Furthermore, the hybrid material of HBS20 has the lowest T_g of 24.0°C, but this is raised to a higher temperature of 30.7°C with 30 mol% of 3-MPS introduced into the system. This was due to the presence of a small amount of rigid Si–O–Si structure formed via the sol–gel process, which may reduce the mobility of nearby organic chains. The inorganic Si–O–Si structure was insufficient for the development of a matrix to enable the hybrid system to become more rigid in HBS20. In addition, the process of acid catalysis would pull the organic side chains (silane group on 3-MPS) together for a sol–gel reaction to form a tiny a Si–O–Si structure. It also made a greater contribution to prohibiting the organic chain segments from coming together and increased the free volume around the stretched chain segments for further chain movement. Consequently, the T_g of the system decreased. Moreover, the T_g that increased as 3-MPS content increased from 20 to 30 mol%, which resulted from the matrix of the inorganic Si–O–Si structure, formed and raised the crosslinking density of whole hybrid system. Furthermore, it resulted in a decrease of molecular mobility and an increase of T_g [22]. Besides, it is interesting to notice that there a wider glass transition region existed in HBS40, which indicates the occurrence of micro-phase separation. This viewpoint will be further discussed with the NMR results.

The other point of interest is that the hybrid system with more than 50 mol% 3-MPS introduced to the copolymer changed its outward appearance to opaque and two T_gs

Table 1
Molecular weight and polydispersity of desired copolymers

Copolymer[a]	$\overline{Mn}$	$\overline{Mw}/\overline{Mn}$
p-MABE	14,600	2.27
MBS20	14,200	2.31
MBS30	14,900	2.25
MBS40	15,600	2.61
MBS50	16,100	2.49
MBS60	17,500	2.43
MBS70	16,400	2.52
MBS80	16,000	2.21
p-MPS	16,900	2.68

[a] These copolymers (MBS20 to MBS80) were synthesized with 3-MPS content of 20, 30, 40, 50, 60, 70, and 80 mol%, respectively.

Table 2
Results of DSC measurement (T_g) and appearance of these hybrid materials

Hybrid materials	Glass transition temperature (°C)[a]		Appearance of the samples
p-MABE	28.1		Transparent and smooth
HBS20	24.0		Transparent and smooth
HBS30	30.7		Transparent and smooth
HBS40	28.9[b]		Light white, translucent, and smooth
HBS50	30.8	40.6	White, opaque, and rough surface
HBS60	27.2	41.7	White, opaque, and rough surface
HBS70	27.3	47.1	White, opaque, and rough surface
HBS80	26.9	49.3	White, opaque, and rough surface
HBS100	25.3	57.2	White, opaque, and rough surface

[a] The hybrid materials with more than 50 mol% of 3-MPS introduced to the system shown two T_g(s).

[b] There was a much wider glass transition region existing in HBS40.

existed in the DSC thermo-scan. The second T_g (the lower one) of the hybrid materials with 50 to 100 mol% 3-MPS introduced into the copolymers was around 27.0°C and approximately the same as the T_g of p-BMA. In addition, the first T_g (the higher one) was increased from 40.6 to 57.2°C when the 3-MPS content was increased from 50 to 100 mol%. It is obvious that the hybrid materials were composed of an acrylic polymer chain and the inorganic Si–O–Si networks in this system. However, the behavior of the glass transition was only influenced by the organic polymer chains in this temperature region. Consequently, the appearance of two T_gs can be attributed to the fact that there were two different organic chain segmental surroundings in these hybrid materials. Actually, with higher silane content, the phase of inorganic Si–O–Si structure occupied more volume and an inorganic matrix was formed. Moreover, it began to confine the organic chain segments and a higher T_g value can be found for these segments. Thus, it can be concluded that a portion of the acrylic polymer chains was limited by inorganic Si–O–Si networks, and exhibited different chain mobility to unconfined polymer chains. These results will be further discussed with the data of $T_{1\rho,H}$ investigation via solid-state NMR.

3.2. ^{13}C CP/MAS NMR spectra

Fig. 2 shows the ^{13}C CP/MAS NMR spectra of synthesized hybrid materials and the BMA homopolymer (p-BMA). The assignments are also made on the figure. The ^{13}C signals of carbonyl groups (ca. 177.7 ppm) and carbon atoms at the main chain (45.4 and 56.2 ppm) were well resolved, and this can be further used for the investigation of molecular environments and chain mobility for the respective segments in these materials.

It is interesting to notice that p-BMA and all the hybrid materials have a unique chemical shift of the carbonyl groups but still there are some tiny differences. From Fig. 3, which shows ^{13}C NMR spectra at a chemical shift of 190–170 ppm, it can be easily seen that the carbonyl resonance peaks were shifted to low field from 177.7 (for p-BMA) to 179.2 (for HBS100) ppm with the increase of 3-MPS content. By Lorentzian curve fitting, the carbonyl peak of these hybrid materials can be split into two peaks with chemical shifts at ca. 177.7 and 179.5 ppm. The rising of the new chemical shift at 179.5 ppm was due to the formation of hydrogen bonds from Si-OH groups at the organic–inorganic interface. With this interaction between hydroxy and carbonyl groups, the unpaired electrons on the oxygen atom (on the carbonyl group) orientate to the hydrogen atom (on the hydroxy group) and reduce the electron density around the carbonyl group. Therefore, the deshielding effect becomes important for the peak of resonance located at low field. With higher silane content, furthermore, the content of the silanol group was increased and the ratio of the hydrogen bonded carbonyl group was increased even in HBS100, hence the chemical shift of the carbonyl groups was totally to low field.

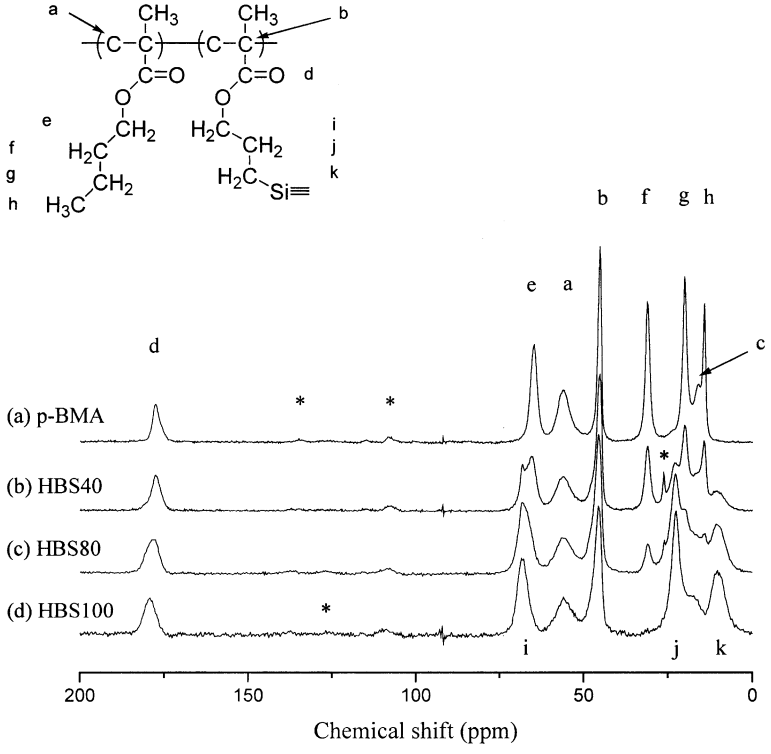

Fig. 2. ^{13}C CP/MAS NMR spectra of (a) p-BMA, (b) HBS40, (c) HBS80, and (d) HBS100. The assignments were made on the figure. The spinning sidebands were also denoted by asterisks.

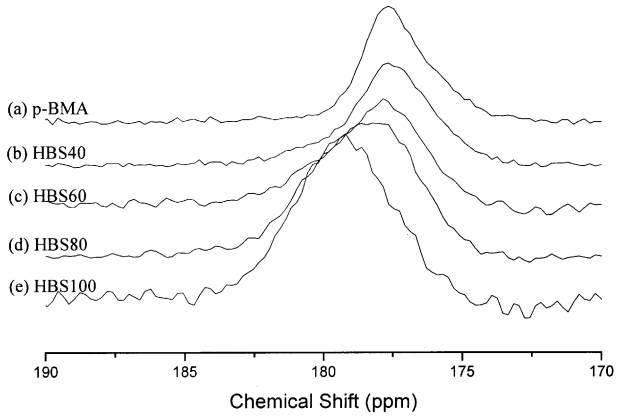

Fig. 3. ^{13}C NMR spectra of carbonyl group in (a) p-BMA, (b) HBS40, (c) HBS80, and (d) HBS100, respectively, at chemical shift of 190–170 ppm.

3.3. Line width and T_2

Via cross polarization from protons to carbons, the proton magnetization at the end of the evolution period is transformed into the amplitude modulation of the ^{13}C signal, which can be probed in the T_2 domain of the material. Hence, the MAS residual line width of the designated peak has T_2 relaxation time inversely proportion to ^{1}H under strong proton decoupling [23–25]. It is sensitive to low frequency motion (only a few kHz), originally from the anisotropic reorientation motion of materials. Thus, the peak width can provide information about the chain interaction, intermolecular coupling, or bond formation on the molecular level. In recent reviews [24–26], it was suggested that the variation of phase structure is the explanation for the chemical shift distribution change.

Half height width of designated NMR shift peaks (at 45.2, 56.3, and 177.7 ppm) was measured for all the materials and is shown in Table 3. It was found that the half height width of all these resonance peaks exhibited a higher value with the increase of 3-MPS content, except the carbonyl resonance peak of HBS80. Practically, the carbonyl resonance peak of hybrid materials of HBS60, HBS80, and HBS100, which were much broader than other materials, resulted not only from the motion of molecular chain segments, but also from the formation of hydrogen bonds, as mentioned at last section. Nevertheless, the variation of half height width of main chain carbon indeed indicated that the phase structure had changed with 3-MPS content and the heterogeneity of this hybrid system was increased with the amount of Si–O–Si structure in the system [25]. More discussion about the phase structure will be presented in next section with the measurement of proton spin-lattice relaxation times.

3.4. $T_{1\rho}$ relaxation times of synthesized organic–inorganic hybrid materials

It is well established that $T_{1\rho,H}$ relaxation times can be used to investigated chain mobility and compatibility of the system on a molecular level [16–19]. With an adequate resolution in ^{13}C spectra, it can be used to resolve the component. However, relaxation rates of ^{13}C exhibit the behavior of the individual environment rather than the domain structure. CP, which involves polarization transfer from ^{1}H to ^{13}C and provides a signal at the chemical shift of ^{13}C for us to monitor the desired segments, enables detection of ^{1}H relaxation.

In this study, the ^{13}C signals of quaternary carbon at main chain (45.2 ppm) and carbonyl groups (177.7 ppm) provided a well-resolved chemical shift for $T_{1\rho,H}$ investigation. The normalized intensity (M_τ/M_0) of materials with proton spin lock time (τ) variation can be obtained and semi-logarithmic plotted in Figs. 4 and 5. For a homogeneous system, the ^{1}H magnetization decay of the desired segment as a function of proton spin lock time obeyed single exponential relaxation as following equation [27]

$$M_\tau/M_0 = x\exp(-\tau/T_{1\rho,H}) \quad (1)$$

Thus, the $T_{1\rho,H}$ relaxation time for the designated segment can be obtained. However, according to these results, it can be found that the variation of normalized intensity with the increasing of proton spin lock time for the hybrid materials, with more than 50 mol% 3-MPS introduced into the system, did not follow a single exponential function but a double

Table 3
^{13}C solid-state CP/MAS NMR analysis of synthesized hybrid materials

Hybrid Materials	Quaternary carbon at main chain		Methylene group at main chain (secondary carbon)		Carbonyl group	
	Peak position (ppm)	Half height width (Hz)	Peak position (ppm)	Half height width (Hz)	Peak position (ppm)	Half height width (Hz)[a]
p-MABE	45.2	476	56.3	1768	177.6	1032
HBS20	45.2	660	56.4	2008	177.7	1136
HBS40	45.2	768	56.2	2220	177.7	1240
HBS60	45.6	844	56.3	2484	177.8	1508
HBS80	45.4	952	56.3	2548	178.2	1928
HBS100	45.6	1032	56.0	2404	179.3	1692

[a] The formation of hydrogen bonds in hybrid materials has to be considered.

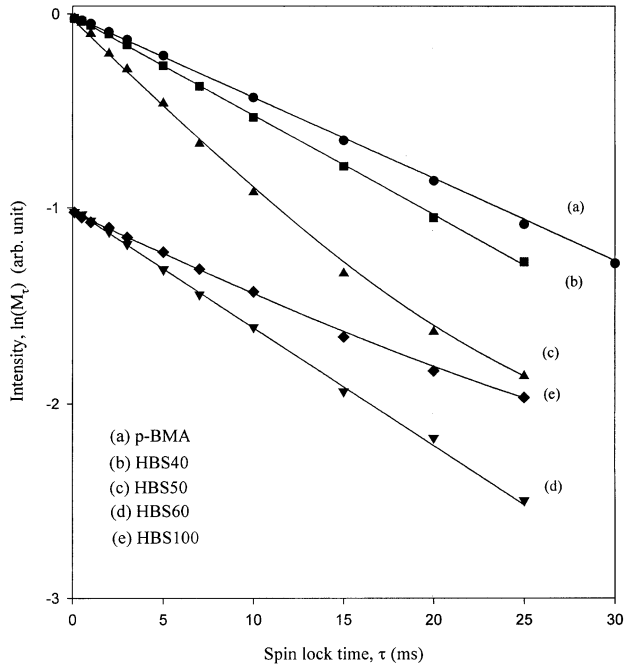

Fig. 4. Semi-logarithmic plots of normalized intensity of main chain carbon (45.2 ppm) versus proton spin lock time for (a) p-BMA, (b) HBS40, (c) HBS50, (d) HBS60, and (e) HBS100. The solid lines, which were suitable fitting to the experimental data, were also plotted in this figure.

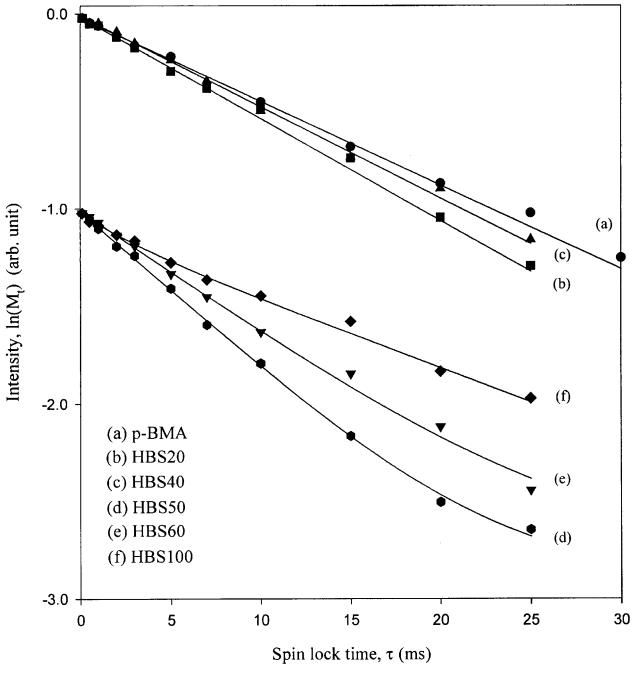

Fig. 5. Plots of the carbonyl normalized intensity (177.7 ppm) versus proton spin lock time for (a) p-BMA, (b) HBS20, (c) HBS40, (d) HBS50, (e) HBS60, and (f) HBS100. Suitable fitting to the experimental data were also plotted by solid lines.

exponential decay, that represented the existence of two relaxation rates of desired chain segment as noted below [25]

$$M_\tau/M_0 = x_a \exp(-\tau/T_{1\rho,H(a)}) + x_b \exp(-\tau/T_{1\rho,H(b)}) \quad (2)$$

where $T_{1\rho,H(a)}$ and $T_{1\rho,H(b)}$ correspond to the relaxation times for two different chain segmental environments. Furthermore, the ratio of x_a to x_b can provide the respective weight fraction of the domains. These two exponential relaxation processes were adequate to describe all the materials in this system. Via suitable exponential decay fitting to the intensity variation, the calculated $T_{1\rho,H}$ relaxation times for the designated chain segments (carbonyl group at 177.7 ppm and quaternary carbon on the polymer backbone at 45.2 ppm) and segmental weight fractions, which corresponded to different $T_{1\rho,H}$ relaxation rates, Table 4 is shown for these hybrid materials.

The quaternary carbon at main chain exhibited a single $T_{1\rho,H}$ relaxation time for p-BMA and most of the hybrid materials except HBS50. With 3-MPS content increased from 0 to 30 mol%, the relaxation rate only slightly decreased from 10.4 to 8.2 ms, which indicated the decrease of chain mobility. However, when the silane content increased to 50 mol%, two relaxation times were found with values of 4.6 and 15.0 ms. With more than 50 mol% of 3-MPS introduced into the system, $T_{1\rho,H}$ relaxation exhibited only a single rate again. On the hand, the carbonyl groups presented a different variation of $T_{1\rho,H}$ relaxation rates to the main chain carbon. With 3-MPS content between 20 to 40 mol%, $T_{1\rho,H}$ relaxation time for carbonyl groups in these hybrid materials exhibited a smaller value than in p-BMA (10.3 ms). In addition, while 3-MPS content in the system increased to more than 40 mol%, the chain segments no longer exhibited a single $T_{1\rho,H}$ relaxation time, but two $T_{1\rho,H}$ relaxation rates, which corresponded to two different chain segmental environments in these hybrid materials. The two distinct $T_{1\rho,H}$ relaxation times, furthermore, diminished with the increase of 3-MPS content.

Homopolymer p-BMA and hybrid materials of HBS20 and HBS30 exhibited similar $T_{1\rho,H}$ relaxation times for main chain carbon and carbonyl groups at side chain, furthermore, the times decreased to a relative low value of 8.2 ms. It means that the domain of the Si–O–Si structure were uniform dispersed and the phase domains in these materials were smaller than ca. 20 Å. Besides, the chain mobility was decreased with the increase of 3-MPS content in the hybrid system, which resulted from the restriction of the dispersed Si–O–Si structure. Although the inference of homogeneity corresponds with the result of DSC analysis on these materials, the change of segmental mobility was not identical with T_g variation tendency completely. It was due to this that NMR investigation is sensitive to segmental mobility around the designated functional groups and differs from T_g thermo-scan by DSC, which describes a larger scale of chain behavior. Hence, a slight difference between $T_{1\rho,H}$ relaxation rates and T_g variations was a reasonable result.

Table 4
$T_{1\rho,H}$ relaxation rates for p-MABE and synthesized hybrid materials with various silane content

Hybrid materials	$T_{1\rho,H}$ values (ms) of desired ^{13}C resonance peak			
	Quaternary carbon at main chain (45.2 ppm)		Carbonyl group (177.7 ppm)[a]	
p-MABE	10.4		10.3	
HBS20	8.9		8.7	
HBS30	8.2		8.4	
HBS40	8.5		9.3	
HBS50	4.6 (94.6)[b]	15.0 (5.4)	5.0 (88.1)	14.3 (8.3)
HBS60	6.7		4.5 (87.4)	11.4 (23.5)
HBS80	8.2		3.9 (37.3)	10.9 (74.9)
HBS100	10.8		3.6 (19.8)	11.8 (79.3)

[a] Quaternary main chain carbon in HBS50 and carbonyl group in hybrid materials, HBS50, HBS60, HBS80, and HBS100, showed two $T_{1\rho,H}$ relaxation rates.
[b] The respective weight fractions of the designated domains, which were obtained from double exponential decay fitting, were also listed in parentheses.

In addition, HBS40 also exhibited only a single $T_{1\rho,H}$ value for the main chain carbon and for carbonyl groups. Nevertheless, these two $T_{1\rho,H}$ relaxation rates were slightly greater than in HBS30 and not quite equal to each other: 8.5 and 9.3 ms for the quaternary carbon at the main chain and carbonyl groups, respectively. It is obvious that micro-phase separation occurred and the domain size would be greater than 20 Å. This inference was also confirmed by the wider glass transition profile of HBS40 in the DSC thermo-scan. At the same time, there is a special case with HBS50, in which there were two $T_{1\rho,H}$ relaxation rates for the quaternary carbon at the main chain. As was discussed, this composition was the beginning of macro-phase separation. Hence, the two molecular surroundings of backbones may be a result of the co-existence of both polymer matrix and Si–O–Si networks during phase inversion, when the developed Si–O–Si networks may confine a portion of organic molecular chain segments and reduce the molecular mobility of restricted chain segments.

It is interesting to note that the relaxation rates of quaternary carbon at the main chain exhibited only single $T_{1\rho,H}$ relaxation rates, which was illustrated by the fact that polymer backbones were all in the same molecular environment except HBS50, but exhibited two $T_{1\rho,H}$ relaxation rates for carbonyl groups with more than 50 mol% 3-MPS in the system. This not only demonstrated the occurrence of macro-phase separation, but also implies that the mechanism of higher main chain mobility with higher 3-MPS content is very complex and need to be discussed further.

With 3-MPS content of 60 to 100 mol% introduced in to the system, $T_{1\rho,H}$ relaxation times of quaternary carbon at the main chain were increased from 6.7 to 10.8 ms. It is obvious that the organic main chains were settled together, and the segmental mobility increased with 3-MPS content (60–100 mol%). However, carbonyl groups at the side chain were divided from two different segmental surroundings. $T_{1\rho,H}$ relaxation times were decreased from 5.0 to 3.6 ms, and from 14.3 to 11.8 ms for the short and long relaxation time components, respectively. Both the hard and soft segments grew more rigid, and the values of respective weight fraction were decreased for the short relaxation time component and increased for the long relaxation time component. It can be determined that the organic main chains and side chains in these materials were located in totally different molecular surroundings.

To begin with, it has to be considered that the organic main chains were all in the same molecular environment, except in the hybrid material of HBS50. When 3-MPS content was less than 50 mol%, mobility of the main chain carbon diminished as 3-MPS content increased. This can be attributed to the uniform dispersed domain of the Si–O–Si structure. On the contrary, with 3-MPS content increased from 60 to 100 mol% in the hybrid system, main chain mobility was raised. Therefore, a deduction can be made that the Si–O–Si structure had changed in these materials and had a different influence from that in the hybrid materials with less than 50 mol% 3-MPS content. In addition, side chain carbonyl groups located at two different segmental surroundings were firmly believed. Hence, an inference can be made that matrix of Si–O–Si networks was developed and the organic chain segments were confined in the matrixes. With this confinement, T_g raised with 3-MPS content is a result that can be expected. However, according to the NMR results, carbon at the main chain obtained higher mobility with a larger amount of silane in the system. It means that a region that is occupied by organic chains provided enough free space for the segmental motion of organic chains. In Fig. 6, it can be seen that with 3-MPS content increased, the amount of T^3 silicon decreased and T^2 and T^1 silicon content increased in the matrix of the Si–O–Si structure, which means that proportion of fully developed matrix of Si–O–Si structure decreased with the increase of 3-MPS content. Consequently, two effects of the inorganic Si–O–Si structure were observed in this study: one was the effect of confinement on chain segments from the rigid Si–O–Si structure that was aside of organic chains; the other was an aggregation of the Si–O–Si structure from sol–gel process, which pulled silane groups together and developed a matrix of Si–O–Si networks. Furthermore, a more flexible organic region

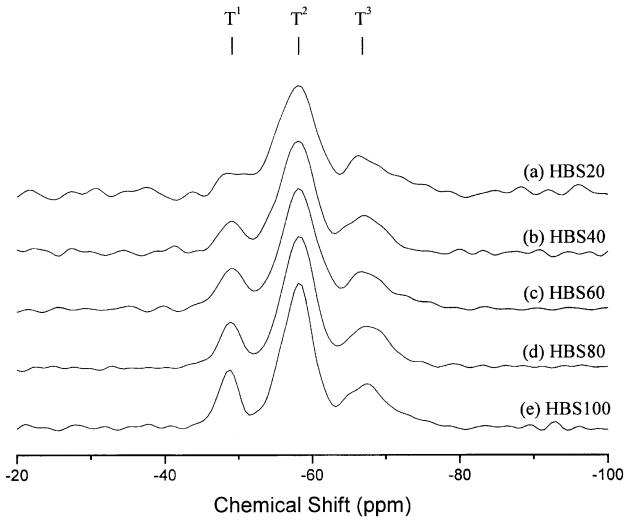

Fig. 6. ^{29}Si MAS NMR spectra of (a) HBS20, (b) HBS40, (c) HBS60, (d) HBS80, and (e) HBS100. The assignments were made on the figure, in which T^1, T^2, and T^3 resonance peaks were at −48.9, −58.2, and −67.1 ppm, respectively.

was created that confined incompletely reacted silane groups. Hence, segmental mobility at a molecular scale exhibited different behavior to macro-scale behavior, as the DSC result determined. Most side chains were dragged to the organic–inorganic interface by the sol–gel reaction, simultaneously. Thus, the lower $T_{1\rho,H}$ relaxation time of the carbonyl groups at the side chains indicated the confinement from the matrix of the Si–O–Si networks and the formation of hydrogen bonding and hence, decreased the mobility of the chain segments. Moreover, the ratio of the fact that the short time component of carbonyl groups was reduced with the rise of 3-MPS content may be attributed to the micro domain that was composed of unfully developed silane groups that had formed in the organic phase [28], furthermore, the influence to reduce the mobility of organic chain segments was diminished. Therefore, respective weight fraction for the long $T_{1\rho,H}$ relaxation time component was increased with 3-MPS content, and the relaxation times were held at ca. 12 ms without further decreasing. This hypothesis can be confirmed by the DSC result of the variation of the second T_g, which was not increased with the increase of 3-MPS content, and also remained at ca. 27°C.

4. Conclusions

BMA homopolymer, HBS20, and HBS30, which have a low silane containing ratio, are homogeneous. In addition, these materials exhibit a decrease in segmental mobility as 3-MPS content increases. With higher 3-MPS content in the hybrid system, micro-phase separation can be found in HBS40 by DSC investigation and $T_{1\rho,H}$ measurement. When the 3-MPS content increases to more than 40 mol%, the hybrid system becomes more complex with the formation of Si–O–Si networks. Two effects of the inorganic Si–O–Si structure can be found: one is the effect of confinement on the chain segments from the rigid Si–O–Si structure; the other is the development of a matrix of Si–O–Si networks via the aggregation of the Si–O–Si structure, which creates a more flexible organic region that confines incompletely reacted silane groups. Hence, segmental mobility exhibits different behavior by T_g investigation and $T_{1\rho,H}$ relaxation rates analysis. Futhermore, increasing 3-MPS content from 50 mol% increases the segmental mobility for organic main chains and decreases it for side chains. The weight fraction of the short time component of carbonyl groups is reduced with the raising of 3-MPS content, which results from the formation of an unfully developed inorganic micro domain in the organic phase, hence, $T_{1\rho,H}$ for the long time component is maintained at ca. 11 ms and the second T_g is also maintained at ca. 27°C

Acknowledgements

The authors are grateful to Dr. Hsin-Lung Chen of Department of Chemical Engineering, National Tsing Hua University, for the use of DSC; and the National Science Council, Taiwan, for their technical support of solid-state NMR.

References

[1] Yoldas BE. J Mater Sci 1977;12:1203.
[2] Yoldas BE. J Mater Sci 1979;14:1843.
[3] Nogami M, Moriya Y. J Non-Cryst Solids 1980;37:191.
[4] MacKenzie JD. J Non-Cryst Solids 1982;48:1.
[5] Brinker CJ, Scherer GW. J Non-Cryst Solids 1985;70:301.
[6] Calvert P. Nature 1991;353:501.
[7] Novak BM. Adv Mater 1993;5:422.
[8] Hoh KP, Ishida H, Koenig JL. Polym Compos 1990;11:121.
[9] Zarzycki J. J Sol–Gel Sci Technol 1997;8:17.
[10] Uhlmann DR, Teowee G, Boulton J. J Sol–Gel Sci Technol 1997;8:1083.
[11] Su CC, Woo EM. Macromolecules 1995;28:6779.
[12] Trollsås M, Kelly MA, Claesson H, Siemens R, Hedrick JL. Macromolecules 1999;32:4917.
[13] Hou S-S, Chung Y-P, Chan C-K, Kuo P-L. Polymer 2000;41:5326.
[14] McBrierty VJ, Douglass DC, Kwei TK. Macromolecules 1978;11:1265.
[15] Stejskal EO, Schaefer J, Sefcik MD, McKay RA. Macromolecules 1981;14:275.
[16] Dickinson LC, Yang H, Chu C-W, Stein RS, Chien JCW. Macromolecules 1987;20:1757.
[17] Jong L, Pearce EM, Kwei TK, Dickinson LC. Macromolecules 1990;23:5071.
[18] Curran S, Kim JK, Han CD. Macromolecules 1992;25:4200.
[19] Cho G, Natansohn A, Ho T, Wynne KJ. Macromolecules 1996;29:2563.
[20] Mark JE, Lee CY-C, Bianconi PA. Hybrid organic–inorganic composites. Washington DC: American Chemical Society, 1995. Chap. 11.
[21] Wei Y, Wang W, Jin D, Yang D, Tartakovskaya L. J Appl Polym Sci 1997;64:1893.
[22] Girard-Reydet E, Lam TM, Pascault JP. Macromol Chem Phys 1994;195:149.

[23] Hagemeyer A, Schmidt-Rohr K, Spiess HW. Adv Magn Reson 1989;13:85.
[24] Schmidt-Rohr K, Clauss J, Spiess HW. Macromolecules 1992;25:3273.
[25] Chu PP, Huang J-M, Wu H-D, Chiang C-R, Chang F-C. J Polym Sci: Polym Phys 1999;35:1155.
[26] Georgi U, Brendler E, Görz H, Roewer G. J Sol–Gel Sci Technol 1997;8:507.
[27] McBrierty VJ, Packer KJ. Nuclear magnetic resonance in solid polymers. Cambridge: Cambridge University Press, 1993. Chap. 2.
[28] Chan C-K, Chu I-M, Lee W, Chin W-K. Submitted for publication.